Hydrotalcite promoted by $NaAlO_2$ as strongly basic catalysts with record activity in glycerol carbonate synthesis

Sreerangappa Ramesh,[a] François Devred,[a] Ludivine van den Biggelaar,[a] and Damien P. Debecker*[a]

A new type of highly basic catalysts is obtained by promoting Mg-Al layered double hydroxides with sodium aluminate. The Mg-Al mixed oxides obtained by the calcination of pristine hydrotalcites are poorly active in the synthesis of glycerol carbonate from glycerol and dimethylcarbonate. Pure sodium aluminate on the other hand is highly active in this reaction, but it is also highly corrosive, making its handling problematic. Remarkably, promoting hydrotalcites with low amount of sodium aluminate is sufficient to reach high yields. At 90°C, with 3 wt.% catalyst and with a DMC:glycerol ratio of 2:1, a glycerol conversion of 92% was achieved after 30 min over the 10 wt. % $NaAlO_2$/hydrotalcite catalyst with almost 100% selectivity towards glycerol carbonate. The texture and the crystallinity of the catalysts were strongly affected by the addition of $NaAlO_2$. Yet the high activity was clearly correlated with the boost in basicity brought about by sodium aluminate promotion. While pristine hydrotalcites possess only weak basic sites, the basicity of the catalysts increased drastically upon promotion with $NaAlO_2$, both in amount and strength. Diffuse reflectance infra-red spectroscopy coupled with CO_2 adsorption show the presence of surface carbonates arising from strongly basic sites. Importantly, our study demonstrates that these basic catalysts are truly heterogeneous, stable, and reusable.

Introduction

The extensive production of biodiesel to fulfill the worldwide demand for greener fuels has resulted in the production of large amounts of glycerol as a byproduct (10 wt.% referred to the amount of biodiesel produced).[1] Since glycerol finds limited applications as a chemical, it has to be converted into value added products in order to make the biodiesel industry more profitable.[2] Glycerol carbonate, for example, has a market value ~10 times higher than crude glycerol. As a nontoxic and water soluble liquid that can be obtained from biomass, glycerol carbonate has become an important platform chemical that can find many applications in personal care products, solvent industry, polymer industry or as a chemical intermediate various other products.[3] Thus, glycerol carbonate synthesis by environmentally benign process and starting from a bio-based product of low value like glycerol is of great interest.[4]

[a] Dr. S. Ramesh, Dr. F. Devred, v.d.B. Ludivine,
Prof. Dr. D. P. Debecker
Institute of condensed matter and Nanoscience,
Université catholique de Louvain Place
Louis Pasteur, 1, box L4.01.09, 1348 Louvain la-Neuve, Belgium.
E-mail: damien.debecker@uclouvain.be

Supporting information for this article is given via a link at the end of the document

Glycerol carbonate can be synthesized from glycerol by four main routes (Scheme 1), namely, by reaction with carbon dioxide,[5] phosgene,[6] urea [7], or alkyl carbonates.[8] The utilization of carbon dioxide to synthesize glycerol carbonate is the most appealing option, but CO_2 activation is challenging and requires harsh reaction conditions.[5a] Glycerol carbonylation with urea can, in principle provide high yields of glycerol carbonate in the presence of heterogeneous acid catalysts, but deactivation of the active sites due to the formation of ammonia as a co-product of the process is a challenge.[7c] A more promising option seems to be available with basic catalysts. For example, Lari et al., reported the continuous production of glycerol carbonate from urea and glycerol.[9] The use of phosgene as carbonylating agent is inadequate due to its environmental hazardous nature. Thus, catalytic reaction of glycerol with alkyl carbonates is considered as the best approach for glycerol carbonate synthesis. In particular, dimethyl carbonate (DMC) is a non-toxic, biodegradable reactant that can be produced via relatively green routes[10] and its transesterification with glycerol is thermodynamically favoured.[8b]

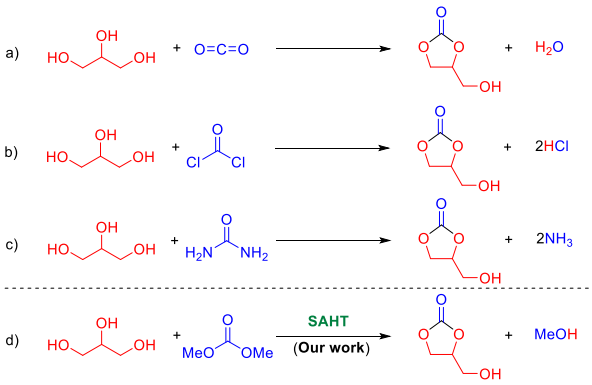

Scheme 1. Glycerol carbonate synthesis by different routes.

Several homogeneous and heterogeneous catalysts were reported in the literature for the transesterification of glycerol with DMC to produce glycerol carbonate.[6] Homogeneous bases, such as KOH, NaOH and K_2CO_3 are efficient catalysts to carry out the above conversion. However, the separation or neutralization of the catalyst from the products is problematic, and large amount of waste water would also be produced during the process.[2b, 3a, 11] Enzyme catalysts showed excellent yields for glycerol carbonate, but they suffer from many drawbacks, such as their high production cost and low reaction rates currently making them unrealistic candidates for such industrial process.[12] Replacement of the traditional homogeneous catalysts, such as KOH, by heterogeneous basic catalysts could reduce waste streams, facilitate catalyst separation from the product, and allow the catalyst to be reused.

Recently, various mixed metal oxides and hydrotalcites-derived compounds have been applied as heterogeneous basic catalysts for the upgrading of glycerol to glycerol carbonate.[13] However, in order to get high yields of glycerol carbonate, the reaction has to be carried out at high temperature (e.g. above 100°C) or with a large excess of DMC to push the equilibrium and the kinetics (e.g. molar ratio of DMC to glycerol of 5).[13c, 14] The basic sites on heterogeneous catalysts are the active centres for the transesterification reaction.[15] Usually, a correlation is found between the basic property (basic strength and amount of basic sites) of the catalysts and their catalytic activity. Hence the development of fine-tuned heterogeneous catalyst exhibiting abundant and strong basic sites is the key for the design of a suitable glycerol carbonate synthesis process.

Layer double hydroxides (LDH), also called hydrotalcites (HT), belong to a class of two dimensional clay materials which received much attention in recent years as catalysts and catalyst supports due to their tunable texture and basicity.[16] It has been shown that activated hydrotalcites can be used as catalysts or catalyst supports in a wide range of base-catalyzed reactions.[16a, 17] However, pristine hydrotalcites or the calcined mixed oxides obtained from them only exhibit moderate activity in the synthesis of glycerol carbonate from glycerol and DMC.[14a]

Sodium aluminate ($NaAlO_2$, or "SA") is a highly basic material and cheaply available in the solid form or as concentrated solution. Being highly insoluble in various organic solvents, $NaAlO_2$ can be used as a true heterogeneous catalyst, especially alcohols. Only a small number of publications have reported $NaAlO_2$ as an active catalyst for a limited number of base-catalyzed reactions (transesterification, isomerisation and condensation).[18] Recently, we showed that $NaAlO_2$ is an excellent active phase for the production of glycerol carbonate, especially when produced by spray drying, in the form of aggregates of small crystallites featuring a high density of strong basic sites.[19] The catalyst exhibited record activity in the classical reaction conditions and was also very active at room temperature.

In its pure solid form, however, $NaAlO_2$ is highly hygroscopic and corrosive, making its handling problematic. Also, the commercially available form of $NaAlO_2$ or the solid obtained by simple drying of $NaAlO_2$ solution has very low surface area (below 5 $m^2.g^{-1}$).[19-20] Blending, supporting or dispersing this highly reactive component would be a relevant strategy to optimize both catalytic activity and workability.

In the present work, we investigate $NaAlO_2$-promoted Mg-Al mixed oxide catalysts obtained by impregnating $NaAlO_2$ onto hydrotalcites, followed by calcination. The new solids are characterized in terms of texture, structure and basic properties. Their performance is measured in the synthesis of glycerol carbonate by transesterification of glycerol with DMC, and their recyclability is studied.

Results and Discussion

Texture, morphology and crystallinity

The pristine hydrotalcite (denoted "HT") had a Mg: Al ratio of 2, a specific surface area (SSA) of 138 m^2g^{-1} and a pore volume (V_p) of 0.50 $cm^3.g^{-1}$ (Table 1). Calcination of hydrotalcites is known to induce dehydration, decarboxylation, loss of compensating anions, and decomposition of lamellar structure leading to MgAl mixed oxides with higher surface area.[16a, 21] Indeed, upon calcination at 400°C (sample denoted "HT400"), the solid reached a SSA of 226 $m^2.g^{-1}$ and a V_p of 0.76 $cm^3.g^{-1}$. The calcined sample showed N_2 physisorption isotherms of type IV (Figure 1) according to the IUPAC classification, characteristic of a mesoporous solids.[22] The formation of mesopores is known to be due to the removal of CO_2 and H_2O from the HT structure.[22-23]

Sodium aluminate was incorporated by impregnation before calcination, with a loading of 5, 10 or 20 wt.% (catalysts denoted 5 SAHT, 10 SAHT and 20 SAHT). In the calcined $NaAlO_2$-promoted catalysts, textural properties were drastically affected. Mesopores were still present and their average size tended to increase (Table1). In parallel, the total pore volume and specific surface area dropped as the $NaAlO_2$ loading increased.

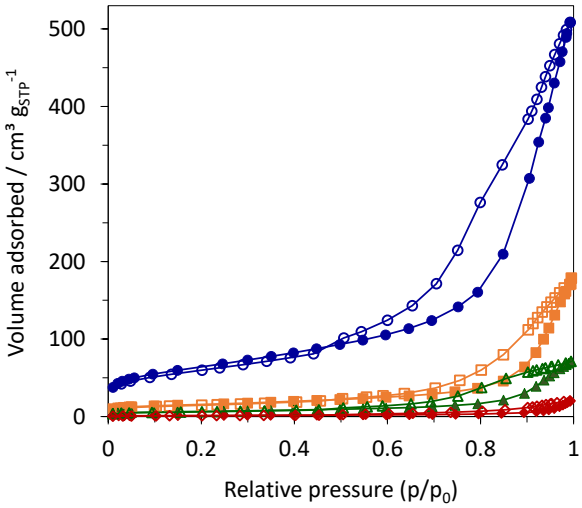

Figure 1. Nitrogen adsorption (full symbols) and desorption (empty symbols) isotherms obtained on HT400 (circles), 5 SAHT (squares), 10 SAHT (tirangles) and 20 SAHT (diamonds).

Table 1. Texture and basicity

Catalyst	SSA ($m^2 g^{-1}$)	V_p ($cm^3 g^{-1}$)	D_p (nm)	Total amount of CO_2 desorbed (mmol g^{-1})	Total amount of CO_2 desorbed ($\mu mol.m^{-2}$)
HT	138	0.50	15	--	
HT400	226	0.76	13	0.5	2.2
5 SAHT	54	0.25	19	0.7	13.0
10 SAHT	23	0.10	18	1.1	47.8
20 SAHT	5	0.03	22	1.3	260
$NaAlO_2$	2	0.01	21	0.8	400

The morphology of the catalysts was inspected by SEM (Figure 2). The hydrotalcite calcined at 400°C showed loose aggregates of the typical platelet structure of calcined hydrotalcites, with a sponge-type aspect. The mesopores described above correspond to the inter particle interstices.[24] Visually, the structure seemed preserved on 5 SAHT but the roughness of the

aggregates seemed to decrease when the $NaAlO_2$ loading was further increased, leading to relatively smooth structures at higher $NaAlO_2$ loading. Also, the aggregated were more compact and inter particle spaces appeared to decrease, indicating that porosity shrunk upon loading SA. Thus, observations from the SEM images were in good agreement with nitrogen physisorption measurements.

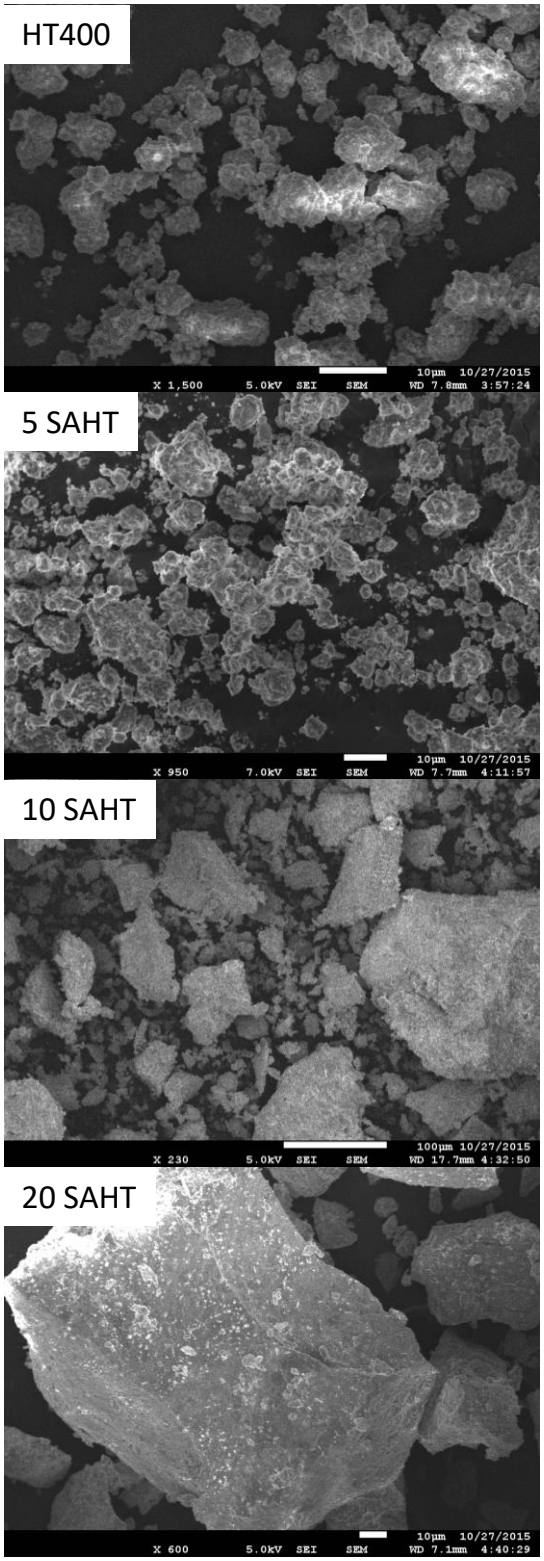

Figure 2. SEM micrographs of the catalysts.

Importantly, the EDX probe mounted on the SEM allowed to map the different elements on the catalyst and to show that $NaAlO_2$ impregnation on the hydrotalcite support was homogeneous, leading to a uniform distribution of the active phase throughout the sample (Supporting Information, Figure S1).

XRD patterns are shown in Figure 3. The pristine hydrotalcite (HT) showed the typical diffractograms of such layered double hydroxide materials, with the peaks at 2θ = 11.2°, 23.0°, and 35.2°, attributed to the d(0 0 3), d(0 0 6), and d(0 1 2) diffraction planes.[16a, 25] After calcination of the pristine support, the crystalline domains of the hydrotalcite are no longer observed and the obtained broad diffraction line of low intensity are ascribed to the MgO-like phase typically formed in calcined LDH.[23] Upon impregnation with $NaAlO_2$ solution, the layered hydrotalcite structure is preserved (10SAHT uncalcined). The destruction of the layered structure is observed upon calcination exactly like in the absence of $NaAlO_2$ (Figure 3). $NaAlO_2$ promoted Mg-Al mixed oxide catalysts exhibited similar diffraction patterns as that of HT400 (Figure 3). At 5 wt.% SA, no additional crystalline species is detected, indicating that sodium aluminate was highly dispersed. The onset of crystalline sodium aluminate was observed for the catalysts with 10 wt.% of $NaAlO_2$. In 20 SAHT, the characteristic peaks of sodium aluminate at 2θ = 20.8°, 30.2°, 33.6°, 35.0°, 45.8°, 48.4°, 51.8°, 58.1°, 61.1°, 63.0° (JCPDS 00-019-1179 and 01-083-0316) were clearly observed.

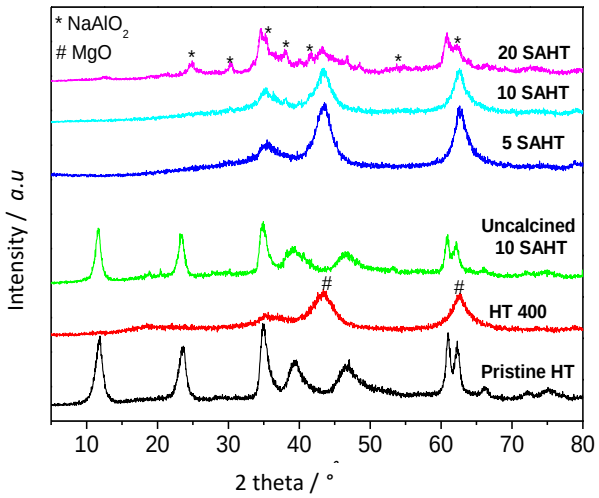

Figure 3. XRD patterns of the pristine and calcined hydrotalcite materials and of the $NaAlO_2$-promoted catalysts with different loading.

Basicity

It is commonly accepted that the catalytic activity for glycerol carbonate synthesis is related to the catalyst basicity; the more basic the catalyst, the higher the activity.[19] The basicity of the prepared catalysts was evaluated using CO_2-TPD measurements (Figure 4). The amount of desorbed CO_2 and the temperature of maximum desorption are the criteria for the amount and strength of basic sites, respectively.[26] In order to evaluate the amount of different types of basic sites, the desorption curve can be arbitrarily differentiated into two regions corresponding to weak and strong basic sites (below or above 400°C respectively). The weak basic sites are related to CO_2 molecules interacting with

surface hydroxyl groups and to Mg^{+2}-O^{-2} and Al^{+3}-O^{-2} pairs. The strong basic sites are related to CO_2 molecules interacting with isolated O^{2-} anions.[16a, 27] CO_2-TPD experiments showed a drastic increase in total basicity upon addition of $NaAlO_2$ (Table 1). In particular, the incorporation of $NaAlO_2$ appears to convert part of the weak basic sites found in bare hydrotalcites into strong basic sites.

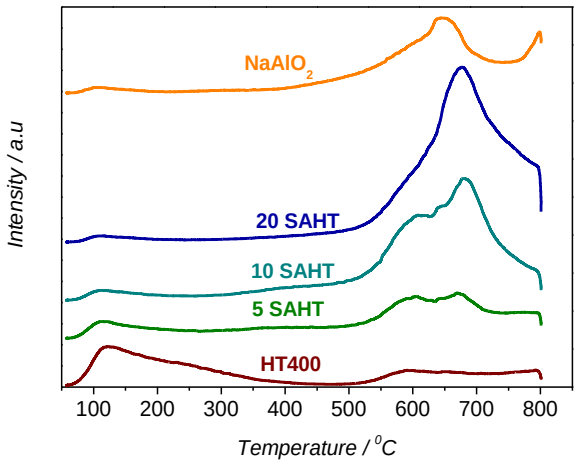

Figure 4. CO_2-TPD of the calcined hydrotalcite (HT400), "x SAHT" catalysts with different $NaAlO_2$ loading, and pure $NaAlO_2$.

To explore further the types of basic sites present on the catalyst, CO_2 adsorption was studied by DRIFTS (Figure 5). The formation of different species of adsorbed CO_2 (monodentate or unidentate, bidentate, and bridged species) stems from the presence of different types of surface basic sites.[28] The CO_2 adsorption modes are shown in Scheme 2. CO_2 adsorbed on oxygen ions with the lowest coordination number (usually monodentate) leads to strong basic sites.[28-29] Bidentate carbonate and bridged carbonate adsorption can be assigned to moderate or weak basic sites. The weak basic sites may also be associated with the surface hydroxyl groups over which the CO_2 adsorption species is present in the form of bicarbonate.[29a] Calcined hydrotalcites show intense peaks at 1636, 1669 and 1684 cm^{-1} which correspond to bridged carbonates which contribute to weak basic sites. Upon addition of sodium aluminate, the bands at 1246 cm^{-1} and 1308 cm^{-1} increased noticeably. The latter correspond to monodentate carbonate attributed to strong basic sites. Strong basic sites clearly increased with the increase in sodium aluminate loading. This is in good agreement with CO_2-TPD results.

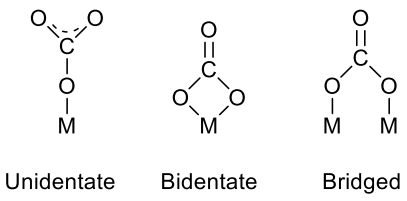

Scheme 2. Different mode of CO_2 adsorption.[28]

Surface analysis

XPS analysis has been carried out in order to obtain information about the surface composition of the catalyst (Table 2). On the bare substrate (HT 400) the presence of Al, Mg, and O was measured in the expected proportions, along with the usual C contamination and with traces of Cl as impurities. The binding energies for Mg (50.0 eV), Al (74.0 eV) and O (531.0 eV) correspond to the expected values for the oxide forms.[30] After $NaAlO_2$ promotion, the surface Na/Mg atomic ratio expectedly increased with the $NaAlO_2$ loading (Table 2).

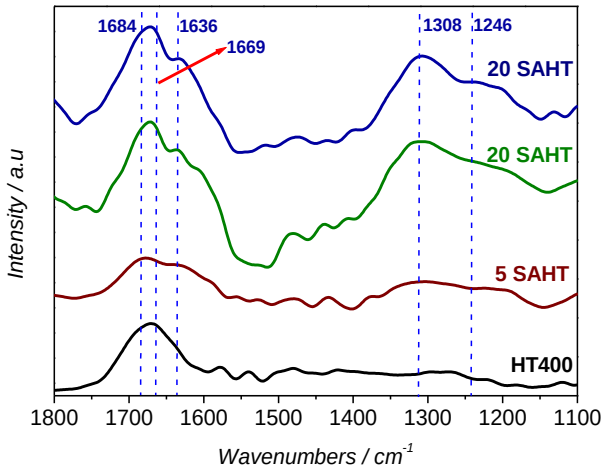

Figure 5. CO_2 DRIFT Spectra of the calcined hydrotalcite (HT400) and of the "x SAHT" catalysts with different $NaAlO_2$ loading.

Table2. XPS analysis of hydrotalcite supported by SA catalysts

Catalyst	Na	Mg	Al	O	C	Cl	Na /Mg ratio
HT400		24.0	12.4	50.8	12.5	0.3	-
5 SAHT	3.9	21.8	14.3	48.5	10.5	0.9	0.18
10 SAHT	7.7	18.5	13.5	45.6	12.9	1.8	0.42
20 SAHT	10.9	10.8	12.6	45.2	18.4	2.1	1.01

Glycerol carbonate synthesis

The catalysts were used in the transesterification of DMC with glycerol to obtain glycerol carbonate at 90 °C. Because an excess of DMC drives the reaction toward the transesterification product, a DMC/glycerol molar ratio of 2 was applied. In all case, 100% selectivity to glycerol carbonate was obtained, as verified by GC and NMR (Supporting Information, Figure S2).

The glycerol conversion as a function of the time is reported in Figure 6. In the absence of a catalyst, only a negligible glycerol carbonate formation was observed after 4 h (yield ~ 5%). Pristine hydrotalcite showed moderate activity, yielding only 26% glycerol conversion after 30 minutes of reaction time at 90°C. Upon calcination, both the textural properties and the basicity are altered. It is known that Brønsted basic sites are converted into Lewis basic sites.[16a] Despite these modifications only slightly higher glycerol conversion is reached (34% after 30 min).

As reported recently,[19] pure $NaAlO_2$ showed much higher activity, almost reaching equilibrium (~93%) after 20 min only. Actually, 58% conversion is already reached after only 5 min of reaction. In the transesterification of DMC with glycerol, the main function of the solid catalyst is to support the abstraction of H^+ from glycerol on the basic sites so as to form glycerol anion.[8b] The higher the catalyst basicity, the more negative the charge of the glyceroxide anion ($C_3H_7O_3^-$), and consequently, the lower the activation energy of the reaction. Hence, the concentration of surface basic sites and strength is known to play an important role in this catalytic reaction.[8b, 19]

Yet, $NaAlO_2$ in its pure solid form is highly hygroscopic and corrosive, and thereby difficult to handle. Hence supporting $NaAlO_2$ on a suitable support was inspected. The 10 SAHT and 20 SAHT catalysts also allows to reach the equilibrium conversion, after a very short reaction time of 30 min. This clearly outcompetes other catalysts from the literature, which sometimes showed similar yield in similar reaction conditions but systematically used either higher catalyst amount or longer reaction time. For example, Granados-Reyes et al. used exactly the same reaction conditions and reached the same equilibrium conversion after 3h with a hydrotalcite catalyst.[31] Similarly, Pan et al. run the reaction at only 70°C but had to use 10 wt.% hydrotalcite catalyst and 4 h reaction time to reach equilibrium.[32] Song et al. reached the same after 4 h of reaction at 95°C and with 10 wt.% of Li/ZnO catalyst.[33] MgO catalyst was also proposed by Simanjuntak et al., reaching 76% conversion in 30 min, at 90°C, with 5 wt.% catalyst.[34] Thus, $NaAlO_2$ blended with hydrotalcite is an excellent alternative, almost allowing to reach the record reaction rates reported for pure $NaAlO_2$ while circumventing the downsides associated with its handling.

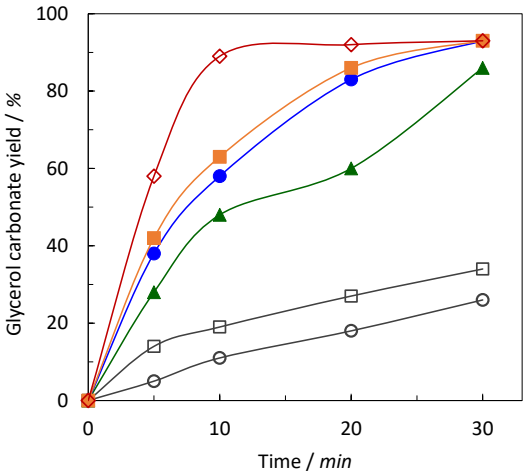

Figure 6. Catalytic activity of fresh pristine hydrotalcite (HT, ○), calcined hydrotalcite (HT400, □), pure $NaAlO_2$ (100SA, ◊)[19] and $NaAlO_2$/hydrotalcite catalysts: 5 SAHT (▲), 10 SAHT (▲) and 20 SAHT (▲). Reaction conditions: glycerol (20 mmol), DMC (40 mmol), 3 wt. % of catalyst (with respect to glycerol), 90°C.

Since all $NaAlO_2$ catalysts similarly allow reaching a high yield after 30 min, it is necessary to look at their initial activity to compare them among each other in terms of intrinsic activity. We approximate initial activity by looking at the glycerol conversion after 5 min of reaction. In these conditions, conversion is as low as 14% with the calcined hydrotalcite. By promoting the hydrotalcite with only 5 wt.% $NaAlO_2$ (5 SAHT), glycerol conversion doubled to 28%. Glycerol conversion increased further to 38% and 42% with further increased in SA concentration to 10 wt.% and 20 wt.% respectively. Thus, intrinsic activity clearly increases with the $NaAlO_2$ loading, consistent with the idea that the main active sites are brought by the strongly basic $NaAlO_2$ active phase. In fact, a correlation is observed between the initial activity and the surface concentration of basic sites (Figure 7).

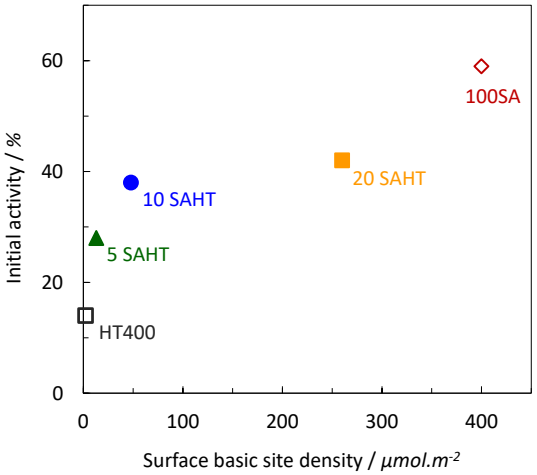

Figure 7. Correlation between the initial catalytic activity and the surface basic site density: calcined hydrotalcite (HT400, □), pure $NaAlO_2$ (100SA, ◊)[19] and $NaAlO_2$/hydrotalcite catalysts (5 SAHT (▲), 10 SAHT (▲), 20 SAHT (▲)).

Stability, reusability and scalability

In order to investigate the heterogeneous nature of the SAHT catalysts, a hot filtration test was conducted to check for the absence of reactivity in solution. The reaction was carried out using 10 SAHT and interrupted after 10 min (conversion = 58%, far enough from the thermodynamic equilibrium). The hot reaction mixture containing the catalyst was filtered to remove the catalyst. The filtrate was refluxed at 90 °C for an additional 50 min in the absence of the solid catalyst. Analysis of the final reaction mixture showed that the conversion did not evolve (Figure 8). This test confirms that there was no leaching of the active sites into the reaction mixture or in other words that the catalysis is truly heterogeneous.

Additionally, to evaluate the recyclability and reusability of the SAHT catalysts, we performed several cycles of reaction. After each run, the catalyst was filtered off, washed twice with 5 mL of methanol to remove the adsorbed reactants on the catalyst surface, and dried at 120 °C for 4 h. The results presented in Figure 9 indicate that the catalyst can be recycled and reused up to three times with no significant loss in catalytic activity. The structural, textural and chemical integrity of the spent catalyst was also examined by X-ray diffraction, N_2-physisorption and CO_2-TPD. XRD diffractograms matched well with the characteristic peaks of fresh catalyst indicating no change in the structure of the catalyst even after three consecutive cycles (Figure S3). Texture and basicity of the used sample (10 SAHT) were not affected either (Table S1).

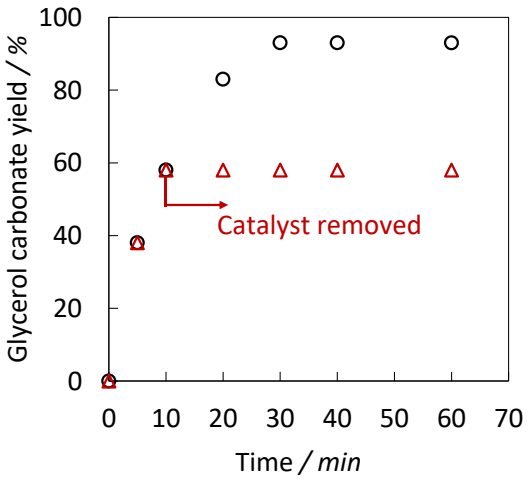

Figure 8. Glycerol carbonate yield as a function of time with 10 SAHT catalyst (circles) and results of the hot filtration test where the catalyst was removed by filtration after 10 min (triangle)**.** Reaction conditions: glycerol (20 mmol), DMC (40 mmol), 3 wt. % of 10 SAHT catalyst (with respect to glycerol), 90°C**.**

Finally, the reaction was conducted at a larger scale to verify if similar levels of performance can be obtained upon scale up. 200 mmol of glycerol (18.4 g) were reacted with 400 mmol of DMC (36.0 g) at 90°C in the presence of 0.55 g of 10 SAHT catalyst (i.e. keeping the same ratios of reactants and catalyst but multiplying all quantities by 10). Exactly the same glycerol conversion was obtained (93%), which can be seen as encouraging in the perspective of scale up to commercial applications of the catalyst for this reaction.

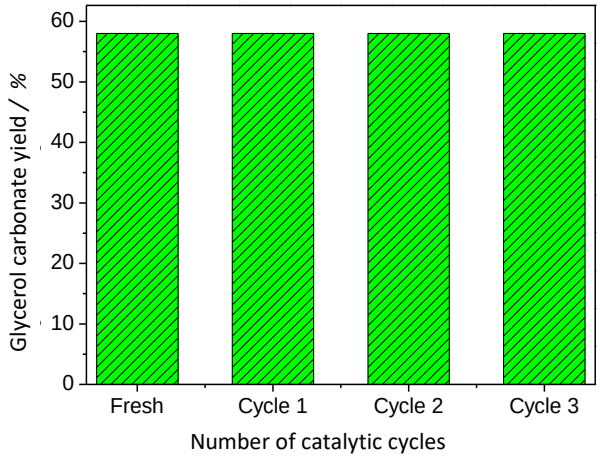

Figure 9. Catalyst reusability studies. Reaction conditions: glycerol (20 mmol), DMC (40 mmol), 3 wt. % of 10 SAHT catalyst (with respect to glycerol), 90°C for 10 min.

Conclusions

We designed a new class of heterogeneous highly basic solids by blending sodium aluminate with hydrotalcite derived mixed oxides. Pure sodium aluminate showed high activity for the reaction but is very difficult to handle due to its highly hygroscopic and corrosive nature. Supporting this highly reactive component on hydrotalcite is shown to be a relevant strategy to optimize catalytic activity and practicability. The method presented here is very simple, based on an impregnation method, followed by calcination. The texture of the hydrotalcite is strongly affected after blending with $NaAlO_2$. The structure of the composite catalyst resembles that of calcined hydrotalcites, with the typical destruction of the layered structure and the appearance of an MgO-like phase. In addition, $NaAlO_2$ crystallites are detected when the loading reaches 10 wt.% or more. Most importantly, the blending with $NaAlO_2$ results in the genesis of abundant strong basic sites. All in all, the catalysts showed full selectivity and high activity in the synthesis of glycerol carbonate from glycerol and DMC. They outperform previously reported heterogeneous catalysts used in similar reaction conditions. They truly act as a heterogeneous catalyst and show excellent reusability and stability. Being both easy to handle and highly active, they constitute a promising alternative to current heterogeneous catalysts for this reaction and other base-catalyzed reactions.

Experimental Section

Chemicals

The pristine hydrotalcite sample (Mg: Al ratio 2) was kindly provided by Kisuma chemicals (The Netherlands). Sodium aluminate solution (25 wt. %) was kindly provided by Dequachim (Belgium). Glycerol (99 %), Ethanol (99 %), Butanol (99 %), Dimethyl carbonate (99 %) and Glycerol carbonate (90%) were obtained by Sigma Aldrich and were used as received.

Catalyst preparation

A series of $NaAlO_2$-promoted Mg-Al mixed oxides catalysts with $NaAlO_2$ content from 0 to 20 wt.% was prepared by an impregnation method. The required quantity of $NaAlO_2$ solution (25 wt.% in water) was diluted in distilled water (10 ml) and this solution was added to 5 g of hydrotalcite support with continuous mixing, to form a thick paste. Excess water was removed by evaporation on water bath. The resulting solid was dried at 100 °C overnight and finally calcined at 400 °C for 4 h in a static air muffle furnace. These catalysts were denoted as "xSAHT", where x indicates the weight content of $NaAlO_2$ (“SA”) in the final mixed oxide (in wt.%). The pristine hydrotalcites material is denoted "HT" and the calcined hydrotalcites (that has not undergone the impregnation steps) is denoted "HT400". A pure $NaAlO_2$ catalysts (100SA) was prepared by spray drying, as recently reported.[19]

Catalyst characterization

X-ray diffraction (XRD) powder patterns were collected on a Siemens diffractometer model D5000 fitted with a Cu Kα (1.541˚) radiation source. Data were recorded over a 2Θ range of 10–80° with an angular step of 0.05° at 3 s/step which resulted in a scan rate of 1°/min. Patterns were identified using files from the Joint Committee on Powder Diffraction Standards (JCPDS). Textural properties were determined by nitrogen physisorption at 77 K using a Micromeritics Tristar equipment. Samples were previously degassed in situ at 393 K under vacuum for overnight. Surface areas were calculated using the Brunauer–Emmet–Teller (BET)

methods over a p/p_0 range where a linear relationship was maintained (0.05-0.30).

To evaluate the basicity of the prepared catalysts, CO_2 temperature-programmed desorption (TPD) experiments were conducted using a CATLAB instrument, from Hiden equipped with QGA mass spectrometer for gas analysis. Approximately 60 mg of each sample were loaded in a quartz micro-reactor supported by quartz wool and degassed at 500°C for 1h using a heating rate of 10°C/min in flowing helium (50 cm^3min^{-1}). Next, the samples were cooled to 50°C and exposed to flowing 15% CO_2-He (50 cm^3min^{-1}) for 1.5h and finally purged in flowing helium for 3h at 50°C. In the TPD experiments, the samples were heated up to 800°C using a heating rate of 5°$Cmin^{-1}$ and a He flow of 50 cm^3min^{-1}. The amounts of desorbed CO_2 was obtained by integration of the desorption profiles and referenced to the signals calibrated for known volumes of analyzed gases.

CO_2 adsorption was explored by diffuse reflection infrared Fourier transform spectroscopy (DRIFTS), with a BRUKER EQUINOX 55 spectrometer. The sample was heated to 400 °C in He flow and held at this temperature for 1 h prior to experiment in order to remove absorbed water. Then, it was cooled to 30 °C and 140 scans were recorded and averaged. High-purity carbon dioxide was introduced to the cell at 50 cm^3min^{-1} for 1 h. Then, a He flow of 50 cm^3min^{-1} was admitted and spectra of adsorbed CO_2 were recorded under using a resolution of 4 cm^{-1} (average of 140 scans).

Scanning Electron Microscope (SEM) images were used to determine the morphology of the studied samples. SEM images were taken with a JEOL 7600 F with a 15.0 kV voltage. Samples were dried under vacuum at 60 °C for 24 h and then placed on a piece of carbon black tape on an aluminium stub. A chromium sputter coating of 10 nm was applied under vacuum with a Sputter Metal 208 HR (Cressington).

The XPS analyses were performed on a SSX 100/206 photoelectron spectrometer from Surface Science Instruments (USA) equipped with a monochromatized micro focused Al X-ray source (powered at 20 mA and 10 kV). The sample powder was pressed in small stainless steel troughs of 4 mm diameter and placed on a conductive aluminium carousel. The pressure in the analysis chamber was around 10-6 Pa. The angle between the surface normal and the axis of the analyser lens was 55°. The analysed area was approximately 1.4 mm^2 and the pass energy was set at 150 eV. In these conditions, the full width at half maximum (FWHM) of the Au 4f7/2 peak of a clean gold standard sample was about 1.6 eV. A flood gun set à 8 eV and a Ni grid placed 3 mm above the sample surface were used for charge stabilisation The C-(C, H) component of the C1s peak of carbon has been fixed to 284.8 eV to set the binding energy scale. Data treatment was performed with the Casa XPS program (Casa Software Ltd, UK), some spectra were decomposed with the least squares fitting routine provided by the software with a Gaussian/Lorentzian (85/15) product function and after subtraction of a nonlinear baseline. Molar fractions were calculated using peak areas normalised on the basis of acquisition parameters and sensitivity factors provided by the manufacturer.

Transesterification of glycerol with DMC

Glycerol transesterification with DMC was carried out in a 25 mL round-bottom flask fitted with a water cooled condenser. In a typical experiment, the reaction mixture was prepared by introducing glycerol (20 mmol) and DMC (40 mmol). Then, the reaction was started by adding the catalyst (3 wt. % with respect to glycerol). The reaction mixture was heated to the desired temperature and stirred at maximum speed using an oil bath mounted on a hotplate equipped with a magnetic stirrer and a thermocouple. The reaction was kept under these conditions for the duration of the reaction. After the desired reaction time, the reaction mixture was allowed to cool down to room temperature and 5.0 g of ethanol and 0.2 g of butanol (as external standard) were added to the reaction mixture. After mixing for 3 min, the reaction mixture was centrifuged to separate the solid catalyst.

The reaction products were analyzed by gas chromatography (GC-456 SCION BRUKER) equipped with a flame ionization detector, split/splitless injection unit and a capillary column (DB-WAX, 30 m, 0.25 mm, 0.25 m). Helium was used as the carrier gas. The injection was performed in split mode with a split ratio of 100:1. Initially, the oven temperature was set at 100°C and was increased at the rate of 15°C min^{-1} until it reached 240°C and then it was maintained at this temperature for 15 min. The FID and injector temperatures were fixed at 270°C and 300°C, respectively. The products were confirmed by proton NMR studies (Bruker NMR with 300 mHz instrument by using TMS as standard). The experimental runs were repeated three times and showed good repeatability (maximum deviation of 3% in relative for the conversion).

Acknowledgements

Authors gratefully acknowledge the Walloon Region for the financial support (BEWARE programme, convention n° 1410279).

Conflict of interest

The authors declare no conflict of interest.

Keywords: Sodium aluminate • Layered double hydroxide • Solid base catalysts • Glycerol carbonate

[1] D. T. Johnson, K. A. Taconi, *Environ. Prog.* **2007**, *26*, 338-348.
[2] (a) J. R. Ochoa-Gómez, O. Gómez-Jiménez-Aberasturi, C. Ramírez-López, M. Belsué, *Org. Process Res. Dev.* **2012**, *16*, 389-399; (b) J. C. Serrano-Ruiz, R. Luque, A. Sepulveda-Escribano, *Chem. Soc. Rev.* **2011**, *40*, 5266-5281; (c) T. W. Turney, A. Patti, W. Gates, U. Shaheen, S. Kulasegaram, *Green Chem.* **2013**, *15*, 1925-1931; (d) N. Godard, A. Vivian, L. Fusaro, L. Cannavicci, C. Aprile, D. P. Debecker, *ChemCatChem* **2017**, n/a-n/a; (e) S. Ramesh, N. J. Venkatesha, *ACS Sus. Chem. Eng.* **2017**, *5*, 1339-1346.
[3] (a) K. Hu, H. Wang, Y. Liu, C. Yang, *J. Ind Eng. Chem.* **2015**, *28*, 334-343; (b) H. Li, C. Xin, X. Jiao, N. Zhao, F. Xiao, L. Li, W. Wei, Y. Sun, *J. Mol. Catal. A* **2015**, *402*, 71-78.
[4] J. Liu, Y. Li, J. Zhang, D. He, *Appl. Catal. A* **2016**, *513*, 9-18.
[5] (a) H. Li, D. Gao, P. Gao, F. Wang, N. Zhao, F. Xiao, W. Wei, Y. Sun, *Catal. Sci. Tech.* **2013**, *3*, 2801-2809; (b) J. Zhang, D. He, *J. Chem. Technol. Biotechnol.* **2015**, *90*, 1077-1085; (c) C. Vieville, J. W. Yoo, S. Pelet, Z. Mouloungui, *Catal. Lett.* **1998**, *56*, 245-247.
[6] M. O. Sonnati, S. Amigoni, E. P. Taffin de Givenchy, T. Darmanin, O. Choulet, F. Guittard, *Green Chem.* **2013**, *15*, 283-306.
[7] (a) C. R. Kumar, K. Jagadeeswaraiah, P. S. S. Prasad, N. Lingaiah, *ChemCatChem* **2012**, *4*, 1360-1367; (b) K. Jagadeeswaraiah, C. R. Kumar, P. S. S. Prasad, N. Lingaiah, *Catal. Sci. Tech.* **2014**, *4*, 2969-2977; (c) P. Manjunathan, R. Ravishankar, G. V. Shanbhag, *ChemCatChem* **2016**, *8*, 631-639; (d) K. Jagadeeswaraiah, C. Ramesh Kumar, A. Rajashekar, A. Srivani, N. Lingaiah, *Catal. Lett.* **2016**, *146*, 692-700; (e) S. Sandesh, G. V. Shanbhag, A. B. Halgeri, *RSC Adv.* **2014**, *4*, 974-977; (f) V. S. Marakatti, A. B. Halgeri, *RSC Adv.* **2015**, *5*, 14286-14293.
[8] (a) J. R. Ochoa-Gomez, O. Gomez-Jimenez-Aberasturi, C. Ramirez-Lopez, B. Maestro-Madurga, *Green Chem.* **2012**, *14*, 3368-3376; (b) P. Kumar, P. With, V. C. Srivastava, R. Gläser, I. M. Mishra, *Ind Eng. Chem. Res.* **2015**, *54*, 12543-12552; (c) S. Sandesh, G. V. Shanbhag, A. B. Halgeri, *Catal. Lett.* **2013**, *143*, 1226-1234; (d) F. S. H. Simanjuntak, J. S. Choi, G. Lee, H. J. Lee, S. D. Lee, M. Cheong, H. S. Kim, H. Lee, *Appl. Catal., B* **2015**, *165*, 642-650.
[9] G. M. Lari, A. B. L. de Moura, L. Weimann, S. Mitchell, C. Mondelli, J. Perez-Ramirez, *J. Mater. Chem. A* **2017**, *5*, 16200-16211.
[10] (a) P. Unnikrishnan, P. Varhadi, D. Srinivas, *RSC Adv.* **2013**, *3*, 23993-23996; (b) K. Almusaiteer, *Catal. Commun.* **2009**, *10*, 1127-1131; (c) H. Chen, S. Wang, M. Xiao, D. Han, Y. Lu, Y. Meng, *Chin. J. Chem. Eng.* **2012**, *20*, 906-913.

[11] J. R. Ochoa-Gómez, O. Gómez-Jiménez-Aberasturi, B. Maestro-Madurga, A. Pesquera-Rodríguez, C. Ramírez-López, L. Lorenzo-Ibarreta, J. Torrecilla-Soria, M. C. Villarán-Velasco, *Appl. Catal. A* **2009**, *366*, 315-324.

[12] S. C. Kim, Y. H. Kim, H. Lee, D. Y. Yoon, B. K. Song, *J. Mol. Catal. B* **2007**, *49*, 75-78.

[13] (a) F. S. H. Simanjuntak, V. T. Widyaya, C. S. Kim, B. S. Ahn, Y. J. Kim, H. Lee, *Chem. Eng. Sci.* **2013**, *94*, 265-270; (b) M. S. Khayoon, B. H. Hameed, *Appl. Catal. A* **2013**, *466*, 272-281; (c) P. Liu, M. Derchi, E. J. M. Hensen, *Appl. Catal. A* **2013**, *467*, 124-131.

[14] (a) M. Malyaadri, K. Jagadeeswaraiah, P. S. Sai Prasad, N. Lingaiah, *Appl. Catal. A* **2011**, *401*, 153-157; (b) Z. Liu, J. Wang, M. Kang, N. Yin, X. Wang, Y. Tan, Y. Zhu, *J. Ind Eng. Chem.* **2015**, *21*, 394-399; (c) P. Liu, M. Derchi, E. J. M. Hensen, *Appl. Catal. B* **2014**, *144*, 135-143.

[15] (a) R. Bai, Y. Wang, S. Wang, F. Mei, T. Li, G. Li, *Fuel Process. Technol.* **2013**, *106*, 209-214; (b) J. V. Gerpen, *Fuel Process. Technol.* **2005**, *86*, 1097-1107.

[16] (a) D. P. Debecker, E. M. Gaigneaux, G. Busca, *Chem. Eur.J.* **2009**, *15*, 3920-3935; (b) W. Xie, H. Peng, L. Chen, *J. Mol. Catal. A* **2006**, *246*, 24-32; (c) C. Noda Pérez, C. A. Pérez, C. A. Henriques, J. L. F. Monteiro, *Appl. Catal. A* **2004**, *272*, 229-240; (d) D. Tichit, M. H. Lhouty, A. Guida, B. H. Chiche, F. Figueras, A. Auroux, D. Bartalini, E. Garrone, *J. Catal.* **1995**, *151*, 50-59.

[17] (a) D. Tichit, D. Lutic, B. Coq, R. Durand, R. Teissier, *J. Catal.* **2003**, *219*, 167-175; (b) J. Yu, J. Li, H. Wei, J. Zheng, H. Su, X. Wang, *J. Mol. Catal. A* **2014**, *395*, 128-136.

[18] (a) S. K. Cherikkallinmel, A. Gopalakrishnan, Z. Yaakob, R. M. Ramakrishnan, S. Sugunan, B. N. Narayanan, *RSC Adv.* **2015**, *5*, 46290-46294; (b) T. Wan, P. Yu, S. Wang, Y. Luo, *Energy & Fuels* **2009**, *23*, 1089-1092; (c) A. V. Agafonov, I. A. Yamanovskaya, V. K. Ivanov, G. A. Seisenbaeva, V. G. Kessler, *J. Sol-Gel Sci. Technol.* **2015**, *76*, 90-97; (d) R. Bai, P. Liu, J. Yang, C. Liu, Y. Gu, *ACS Sus. Chem. Eng.* **2015**, *3*, 1292-1297; (e) S. Despax, B. Estrine, N. Hoffmann, J. Le Bras, S. Marinkovic, J. Muzart, *Catal. Commun.* **2013**, *39*, 35-38.

[19] S. Ramesh, D. P. Debecker, *Catal. Commun.* **2017**, *97*, 102-105.

[20] V. Mutreja, S. Singh, A. Ali, *J. Oleo. Sci.* **2012**, *61*, 665-669.

[21] R. Warringham, S. Mitchell, R. Murty, R. Schäublin, P. Crivelli, J. Kenvin, J. Pérez-Ramírez, *Chem. Mater.* **2017**, *29*, 4052-4062.

[22] P. Kuśtrowski, L. Chmielarz, E. Bożek, M. Sawalha, F. Roessner, *Mater. Res. Bull.* **2004**, *39*, 263-281.

[23] S. I. Omonmhenle, I. J. Shannon, *Appl. Clay. Sci.* **2016**, *127–128*, 88-94.

[24] M. Mokhtar, S. N. Basahel, Y. O. Al-Angary, *J. Alloys .Compd.* **2010**, *493*, 376-384.

[25] S. Zhao, H. Yi, X. Tang, F. Gao, Q. Yu, Y. Zhou, J. Wang, Y. Huang, Z. Yang, *Ultrason. Sonochem.* **2016**, *32*, 336-342.

[26] (a) C. Chizallet, G. Costentin, M. Che, F. Delbecq, P. Sautet, *J. Phy. Chem. B* **2006**, *110*, 15878-15886; (b) G. Garbarino, C. Wang, I. Valsamakis, S. Chitsazan, P. Riani, E. Finocchio, M. Flytzani-Stephanopoulos, G. Busca, *Appl. Catal. B* **2017**, *200*, 458-468.

[27] X. Yu, N. Wang, W. Chu, M. Liu, *Chem. Eng. J.* **2012**, *209*, 623-632.

[28] H. Du, C. T. Williams, A. D. Ebner, J. A. Ritter, *Chem. Mater.* **2010**, *22*, 3519-3526.

[29] (a) H. Li, X. Jiao, L. Li, N. Zhao, F. Xiao, W. Wei, Y. Sun, B. Zhang, *Catal. Sci. Tech.* **2015**, *5*, 989-1005; (b) T. Das, G. Deo, *J. Mol. Catal. A* **2011**, *350*, 75-82.

[30] A. H. Padmasri, A. Venugopal, V. Durga Kumari, K. S. Rama Rao, P. Kanta Rao, *J. Mol. Catal. A* **2002**, *188*, 255-265.

[31] J. Granados-Reyes, P. Salagre, Y. Cesteros, *Appl. Clay. Sci.* **2016**, *132*, 216-222.

[32] S. Pan, L. Zheng, R. Nie, S. Xia, P. Chen, Z. Hou, *Chinese J. Catal.* **2012**, *33*, 1772-1777.

[33] X. Song, Y. Wu, F. Cai, D. Pan, G. Xiao, *Appl. Catal. A* **2017**, *532*, 77-85.

[34] F. S. H. Simanjuntak, S. R. Lim, B. S. Ahn, H. S. Kim, H. Lee, *Appl. Catal. A* **2014**, *484*, 33-38.

Entry for the Table of Contents

Layout 2:

FULL PAPER

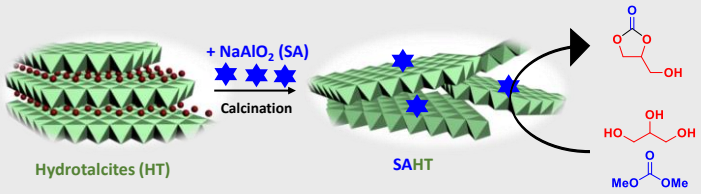

*Sreerangappa Ramesh, François Devred, van den Biggelaar Ludivine, Damien P. Debecker**

Page No. – Page No.

Hydrotalcite promoted by sodium aluminate as highly basic catalysts for glycerol carbonate synthesis

Hydrotalcites are known basic materials but perform poorly in the synthesis of glycerol carbonate. $NaAlO_2$ is highly active but not convenient. Promoting hydrotalcites with low amount sodium aluminate allows to overcome these limitations, leading to excellent catalysts which combine the qualities of the two partners.